J Electroceram (2006) 17:369–373
DOI 10.1007/s10832-006-9009-y

Effects of potential and heat treatment on phase transition of alumina dielectric layer

Han-Jun Oh · Jong-Ho Lee · Hong-Joo Ahn · Yongsoo Jeong · Chang-Hoe Heo · Choong-Soo Chi

Received: 29 June 2005 / Revised: 19 April 2006 / Accepted: 1 May 2006

Abstract The characteristics and growth behaviors of alumina dielectric layer formed by anodic oxidation were investigated. The aluminum oxide layer anodized at 400 V was predominantly amorphous alumina, but at the applied potentials more than 500 V, amorphous and crystalline γ-alumina were existed in anodic oxide layer and the ratio of γ-alumina increased with the increasing applied potential. During the heat treatment at 600°C or higher temperature, amorphous alumina layer was transformed into the crystalline γ-alumina. The phase transition of anodic amorphous alumina into crystalline depends on anodic applied potentials and heat-treatment temperatures.

Keywords Dielectric layer · γ-alumina · Rutherford backscattered spectroscopy · Anodization · Aluminum electrolytic capacitors

H.-J. Oh
Dept. of Materials Science, Hanseo University, Seosan 352-820, Korea

J.-H. Lee
Dept. of Chemistry, Hanseo University, Seosan 352-820, Korea

H.-J. Ahn
Korea Atomic Energy Research Institute, Daejeon 305-600, Korea

Y. Jeong
Korea Institute of Machinery and Materials, Changwon 641-010, Korea

C.-H. Heo · C.-S. Chi (✉)
School of Advanced Materials Engineering, Kookmin University, Seoul 136-702, Korea
e-mail: cschi@kookmin.ac.kr

1 Introduction

The shape and properties of anodic aluminum oxide film depend on a number of factors, particularly the nature of the electrolytes. In acidic or alkali solutions porous-type film is produced [1, 2], while in neutral electrolytes barrier-type film [3, 4] is generated. In general, dielectrically compact barrier film for electrolytic capacitors [5] is fabricated by anodization with electrolytes in the pH range of 5 to 7. The structure of the film is mostly amorphous, and the chemical composition has a variation in the film. Recently with miniaturization of electronic articles and for energy saving, the need for high voltage films is rapidly increasing. Accordingly attention has been paid to the study on growth behavior and fabrication of the oxide film. For anodic alumina dielectrics, crystalline film has not only a higher density and stable microstructure compared with amorphous film, but also improves the capacitance because of higher dielectric constant [6]. However, much efforts are directed toward increasing the specific surface area by etching techniques [7–12]. And few reports have been found on the microstructure and characteristics for the dielectric film. Therefore, this study have been focused on the growth behavior and stoichiometry of the anodic oxide film, and transition phenomena from amorphous to crystalline phase by heat treatment in order to produce a dielectric layer with high capacitance for electrolytic capacitors.

2 Experimental

Anodization was performed on a highly pure aluminum sheet (99.98%) with a size of 25 mm × 40 mm and thickness of 300 μm. As a pretreatment, a specimen was degreased in NaOH for 3 min, rinsed with deionized (DI) water, and neutralized in HNO_3 bath for 30 s, followed by drying with a stream of air

and electropolishing in a perchloric acid/methanol mixture at 20 V for 5 min. Dielectric oxide film was prepared on the aluminum substrate by anodic oxidation at a constant voltage in boric acid. In the initial stage a constant current density of 25 mA/cm^2 was applied, resulting in a rise of anodic voltage. And when the voltage reached a predetermined value, the constant current mode switched to a constant voltage, at which anodic oxide film was formed for 10 min in boric acid of 95 g/L at 90°C.

Crystallographic identification of anodic oxide film was carried out using X-ray diffraction (Philips, PW1710) with Cu K_α radiation and scanning angle 2θ from 15 to 75°. Phase transition and morphological features were examined with transmission electron microscope (JEOL 1210), using ultramicroscopy. The RBS measurement was conducted by irradiating with $4He^{2+}$ at 2 MeV, for which a tandem-type accelerator (6SDH-2Pelletron) was employed. The scattered particles were detected at a 170° scattering angle to the incident beam direction normal to the oxide film on aluminum substrate. The energy distributions of the scattered ions were accumulated in 1024 channel spectra. From the measured spectrum simulation was carried out using Rump program [13].

3 Results and discussion

3.1 Characteristics of the anodic film

Figure 1 shows the RBS analysis on the alumina film anodized in boric acid of 95 g/L at 100 V, 150 V, 300 V, and 500 V, in which a dotted line represents measured data and a solid one the simulated result. As illustrated in Fig. 1, it is evident that the channel width for the aluminum is increasing gradually, suggesting that the higher the supplied voltage is, the thicker the oxide layer becomes. From the analysis the thickness of the anodic oxide layer is 120, 170, 330, and 510 nm for the applied voltage of 100, 150, 300, and 500 V respectively. When converted into the film growth rate to the voltage, it turns out to be 1.2 nm/V for 100 V, 1.13 nm/V for 150 V, 1.1 nm/V for 300 V, and 1.02 nm/V for 500 V. The values are in agreement with those reported for the growth rate of oxide film according to applied potentials, which is in the range of 1.1 to 1.5 nm/V [14]. For the rate of anodic alumina layer obtained in this work the values revealed the decreasing tendency with the increasing applied voltage. The results are responsible for the variety of specific densities of barrier-type alumina layer, which are known to be 3.2 g·cm^{-3} for amorphous oxide and 3.8 g·cm^{-3} for crystalline [6]. And as shown in this work, crystallization of amorphous oxide during anodization accelerates as the applied potential increases. For the growth rate of the layer due to crystalline structure, there have been reported to be 1.3 to 1.7 nm/V for amorphous oxide films and 0.8 to 1.3 nm/V for crystalline [15].

An analysis was conducted from Fig. 1(b) on the stoichiometry of Al and O elements in the oxide film formed at 150 V. Figure 2 shows a cross sectional TEM image for the film and the measured locations for chemical composition. And as listed in Table 1, it is found that the average thickness of the layer formed at 150 V is 225 nm. The stoichiometric ratio of Al/O is estimated to be 45.9/54.1 at the distance of 40 nm from the interface between the oxide and the aluminum substrate, 41.4/58.6 at 100 nm, and 33.2/66.8

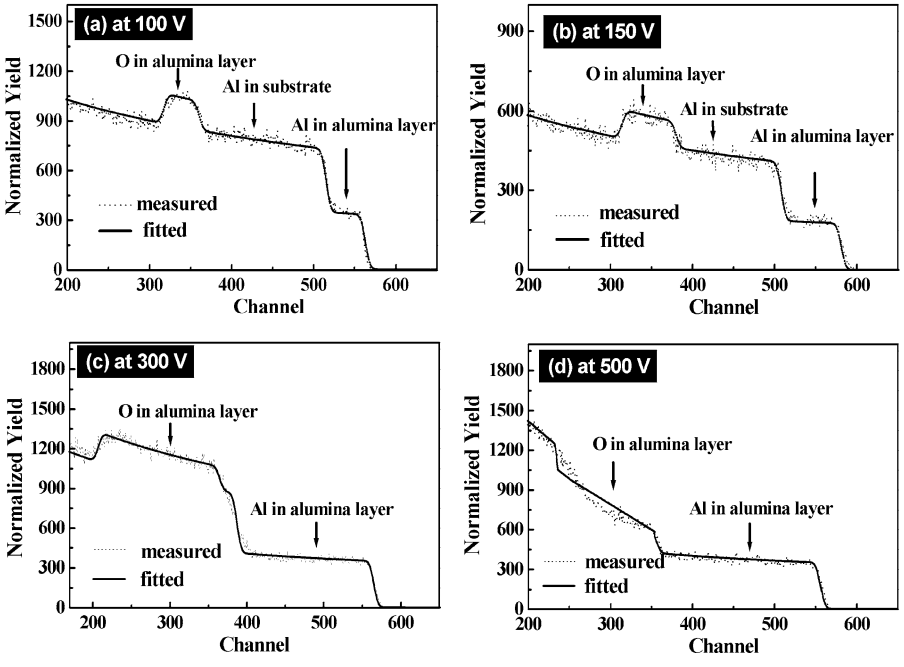

Fig. 1 RBS spectra obtained from the alumina dielectric layers formed on aluminum substrate and fitted results of Rump simulation. The alumina dielectric layers formed by anodization at (a) 100 V, (b) 150 V, (c) 300 V, and (d) 500 V for 10 min in boric acid

Table 1 Stoichiometric ratio of Al and O elements in depth obtained from analysis of the RBS spectrum for the anodic oxide layer formed by anodization at 150 V for 10 min

Location No.	Distance from interface (nm)	Atomic percent (%)	
		Al	O
1	40	45.9	54.1
2	100	41.4	58.6
3	180	33.2	66.8

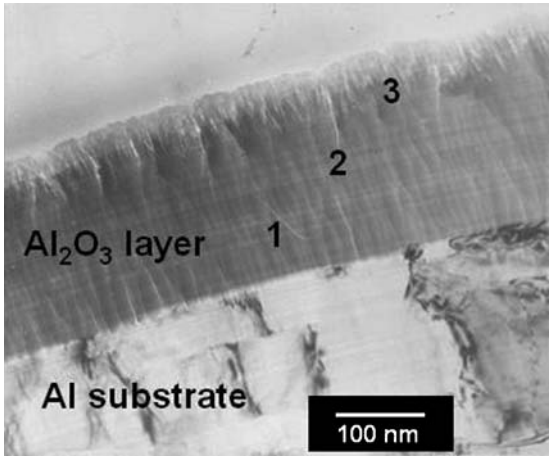

Fig. 2 TEM image of the Al_2O_3 layer formed by anodization at 25 mA/cm^2 for 150V

at 180 nm. If barrier-type anodic alumina layer of Al_2O_3 was ideally formed by anodizing, the overall stoichiometric ratio of Al/O elements in the oxide should be indicated to be 2/3. At the central area of the anodic film the ratio is in good accord with the ideal as represented in Table 1, but at the upper and lower areas the values are deviated from the ideal.

According to the growth mechanisms of anodic oxide layers [16, 17], Al^{3+} from aluminum substrate migrates outward to the direction of electrolyte/oxide interface through oxide layer because of strong electric field by an applied voltage, and, likewise, O^{2-} incorporated into the layer from electrolytes moves inward to the aluminum substrate. Al^{3+} and O^{2-} ions transported from each side combine to form Al_2O_3 in the mid area of the existing oxide, and, as further reaction takes place, the product layer becomes thicker. In the results of this work, a slight deviation from the ideal stoichiometric ratio was observed at both interfaces, compared with that at the mid region of oxide layer.

It is suggested that there is not only the mobility difference of Al^{3+} and O^{2-} under the electric field, but also the diffusion behaviors of the ions which cannot occur ideally since a lot of Al^{3+} and O^{2-} are produced in the substrate/oxide and oxide/electrolyte interfaces respectively. As can be seen in Table 1, this work exhibits that in the area of oxide/electrolyte interface the Al/O ratio is lower than the ideal value of 2/3,

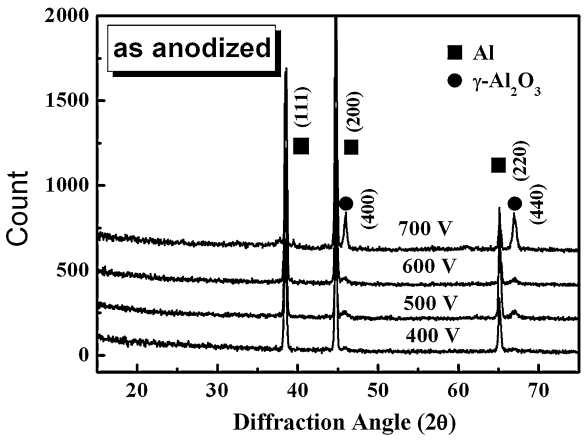

Fig. 3 XRD results of alumina dielectric layers formed at various applied potentials

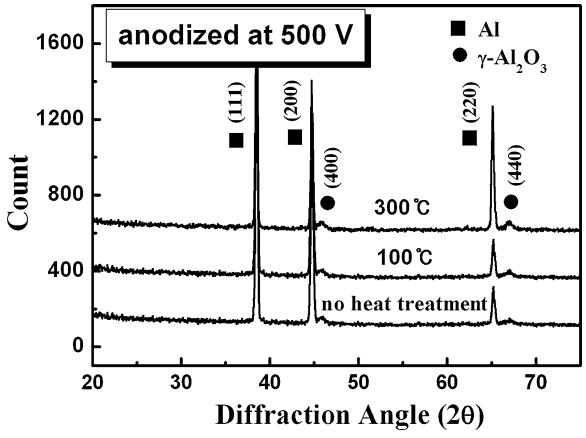

Fig. 4 X-ray diffraction patterns of alumina films anodized at 500 V after various heat treatments

and on the other hand in the substrate/oxide interface higher than that. And in the central region the ratio is in consistent with the ideal. For the stoichometry change in terms of mobility and diffusion of transport ions during anodization, further studies have been proposed [18, 19].

3.2 Applied voltage and crystalline structure

Figure 3 shows XRD patterns of the oxide films prepared by anodization for 10 min at various voltages to investigate the effect of applied voltages on the crystallinity of the oxides. For the film formed at 400 V, only aluminum peak is detected from the substrate, revealing no other crystalline structures. It is found that the dielectric oxide film formed at lower than 400 V is amorphous alumina. However, for the film formed at more than 500 V, γ-alumina crystalline peaks begin to appear in weak intensity. As the voltage increases, the γ-alumina peaks become strong, and for the applied voltage of 700 V are shown distinctly. Accordingly it is predicted that the anodic

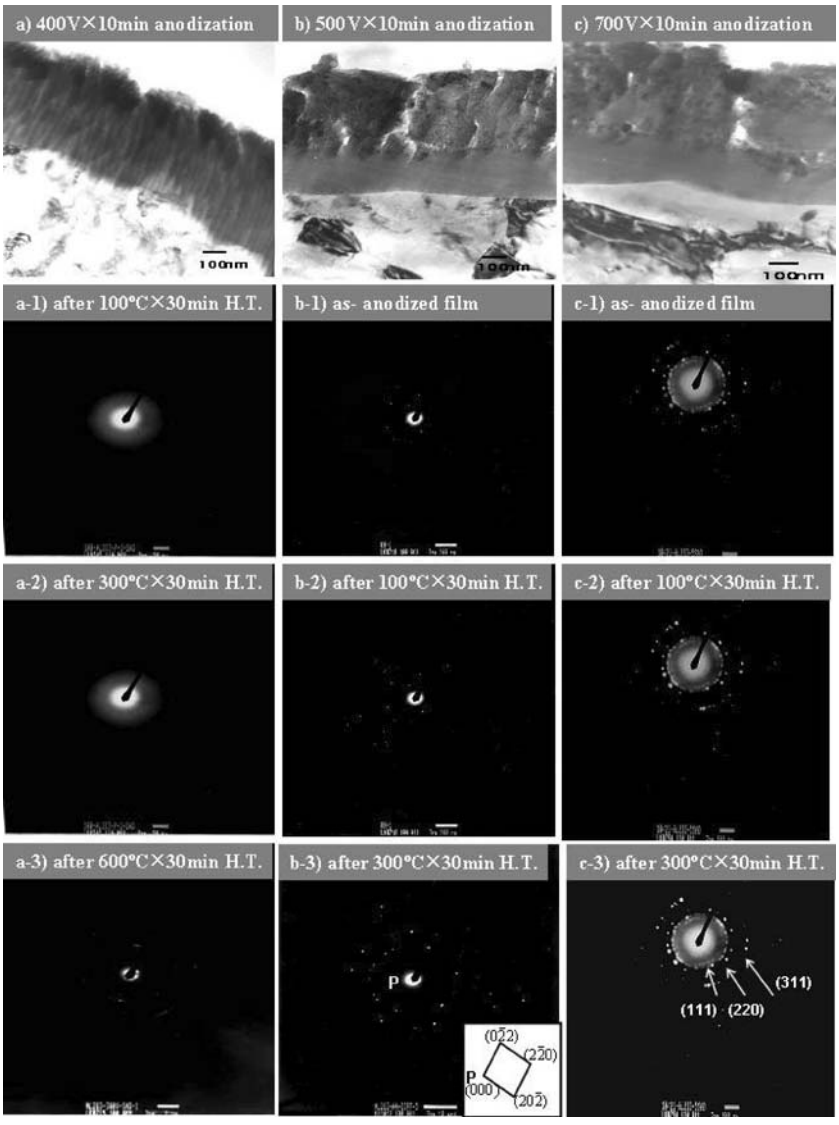

Fig. 5 TEM micrographs of alumina dielectric layers anodized at (a) 400 V, (b) 500 V, and (c) 700 V on aluminum substrate and SADPs for phase transition after various heat treatments

oxide layer is formed to be amorphous when anodized below 400 V, but it is formed to be crystalline when anodized above 500 V. XRD patterns in Fig. 4 exhibit the change by heat treatments in crystallinity of the films formed at 500 V. Crystalline structure of alumina is obtained from the layer anodized at 500 V without any heat treatments. Also it is confirmed that amorphous alumina can be converted to be crystalline with heat treatments, and the volume fraction of crystalline alumina is increasing with the increasing applied voltages.

Figure 5 shows the cross sectional TEM images and SAD patterns for the oxide films anodized at 400 V, 500 V and 700 V, and heat-treated. The thickness was measured from Fig. 5(a)–(c) according to the applied voltages, from which it is derived that the oxide growth rate is decreasing with increasing applied voltages. The thickness of the film is found to be 420 nm for 400 V, 500 nm for 500 V, and 670 nm for 700 V, and the anodizing ratio is 1.05 nm/V, 1.00 nm/V, and 0.96 nm/V respectively, indicating the ratio is decreasing with the increasing voltages. These results seem in good accord with that of the RBS. And the reason for the low value of anodizing ratio at high voltages is regarded as the fact that, with applying high voltages, the anodic oxide surface is formed irregularly, because electro discharging phenomena and gas evolution take place violently on the surface [20, 21] and such defects cause the decrease in the efficiency of film formation.

As shown in Fig. 5(a-1) and (a-2), the SAD patterns for the film anodized at 400 V and heat-treated at 100 and 300°C consist of diffuse and halo rings, displaying diffraction for amorphous specimens. However ring patterns of (311) and (400) from γ-alumina phase were observed for the film heat-treated at 600°C for 30 min, suggesting the transformation of amorphous phase to crystalline. It can be assumed that Al

and O atoms, which are put in irregular order in film anodized at 400 V, are arranged regularly by heat energy, and result in transforming to γ-alumina. Meanwhile, as illustrated in Fig. 5(b) and (c), for the films formed at 500 and 700 V, crystalline diffraction patterns were obtained without any heat treatments. The volume fraction of the crystalline oxides in the layer increases with increasing temperature of heat treatment, and the intensity of the patterns becomes strong, showing a similar tendency to the XRD result.

4 Conclusion

Growth behavior and stoichiometry of anodic aluminum oxides, and phase transformation by heat treatment have been investigated. For the alumina dielectric film formed by anodization the stoichiometry of Al/O atoms is estimated to almost ideal value of 2/3 in the central region of the film, but deviates from the value as the location goes to the both interfaces. The oxide film anodized at low potentials is found amorphous, but the film formed at more than 500 V consists of a mixture of amorphous oxide and crystalline, and, with the higher voltage applied, the volume fraction of γ-alumina increases. The amorphous dielectric film of anodic alumina was transformed to crystalline γ-alumina by heat treatments at more than 600°C. And the transition to the crystalline depends on the applied voltages and heat-treatment temperatures.

Acknowledgment This work has been supported by the research program of the Kookmin University in Korea.

References

1. P. Neufeld and H.O. Ali, *Trans. Inst. Metal Finish.*, **48**, 175 (1970).
2. J. Hitzig, K. Juettner, W.J. Lorenz, and W. Paatsch, *Corrosion. Sci.*, **24**, 945 (1984).
3. P. Skeldon, K. Shimizu, G.E. Thompson, and G.C. Wood, *Surf. Interface Anal.*, **5**, 247 (1983).
4. Han-Jun Oh, Kyung-Wook Jang, and Choong-Soo Chi, *Bull. Korean Chem. Soc.*, **20**, 1340 (1999).
5. Han-Jun Oh, Jung-Gu Kim, Yongsoo Jeong, and Choong-Soo Chi, *Jpn. J. Appl. Phys.*, **39**, 6690 (2000).
6. H. Uchi, T. Kanno, and R.S. Alwitt, *J. Electrochem. Soc.*, **148**, B17 (2001).
7. R.S. Alwitt, *J. Electrochem. Soc.*, **134**, 1891 (1987).
8. J. Flis and L. Kowalczyk, *J. Appl. Electrochem.*, **25**, 507 (1995).
9. J. Scherer, O.M. Magnussen, T. Ebel, and R.J. Behm, *Corros. Sci.*, **41**, 35 (1999).
10. Y. Li, H. Shimada, M. Sakairi, K. Shigyo, H. Takahashi, and M. Seo, *J. Electrochem. Soc.*, **144**, 875 (1997).
11. L.K. Dyer and R.S. Alwitt, *J. Electrochem. Soc.*, **128**, 82 (1981).
12. K. Hebert and R.C. Alkire, *J. Electrochem. Soc.*, **135**, 2451 (1988).
13. L.R. Doolittle, *Nucl. Inst. Meth.*, **B9**, 344 (1985).
14. P. Skeldon, K. Shimizu, G.E. Thompson, and G.C. Wood, *Surf. Interface Anal.*, **5**, 252 (1983).
15. M. Shikanai, M. Sakairi, H. Takahashi, M. Seo, K. Takahiro, S. Nagata, and S. Yamaguchi, *J. Electrochem. Soc.*, **144**, 2756 (1997).
16. M.A. Paez, O. Bustos, G.E. Thompson, P. Skeldon, K. Shimizu, and G.C.Wood, *J. Electrochem. Soc.*, **147**, 1015 (2000).
17. A.P. Li, F. Muler, A. Birner, K. Niesch, and U. Gosele, *J. Appl. Phys.*, **84**, 6023 (1998).
18. H. Habazaki, P. Skeldon, G.E. Thompson, and G.C. Wood, *Philosophical Magazine B*, **71**, 81 (1995).
19. G.C. Wood, P. Skeldon, G.E. Thompson, and K. Shimizu, *J. Electrochem. Soc.*, **143**, 74 (1996).
20. K. Shimizu and S. Tajima, *Electrochim. Acta*, **25**, 259 (1980).
21. S. Tajima, *Electrochim. Acta*, **22**, 995 (1977).